Trapped Electron Mode Turbulence Driven Intrinsic Rotation in Tokamak Plasmas

W. X. Wang, T. S. Hahm, S. Ethier, L. E. Zakharov, and P. H. Diamond

Phys. Rev. Lett. **106**, 085001 — Published 23 February 2011

DOI: 10.1103/PhysRevLett.106.085001

Trapped Electron Mode Turbulence Driven Intrinsic Rotation in Tokamak Plasmas

W. X. Wang,* T. S. Hahm, S. Ethier, and L. E. Zakharov
Plasma Physics Laboratory, Princeton University, P.O. Box 451, Princeton, NJ 08543, USA

P. H. Diamond
University of California, San Diego, La Jolla, CA 92093, USA

Recent progress from global gyrokinetic simulations in understanding the origin of intrinsic rotation in toroidal plasmas is reported with emphasis on electron thermal transport dominated regimes. The turbulence driven intrinsic torque associated with nonlinear residual stress generation by the fluctuation intensity and the intensity gradient in the presence of zonal flow shear induced asymmetry in the parallel wavenumber spectrum is shown to scale close to linearly with plasma gradients and the inverse of the plasma current. These results qualitatively reproduce empirical scalings of intrinsic rotation observed in various experiments. The origin of current scaling is found to be due to enhanced $k_{\|}$ symmetry breaking induced by the increased radial variation of the safety factor as the current decreases. The physics origin for the linear dependence of intrinsic torque on pressure gradient is that both turbulence intensity and the zonal flow shear, which are two key ingredients for driving residual stress, increase with the strength of turbulence drive, which is R_0/L_{T_e} and R_0/L_{n_e} for the trapped electron mode.

PACS numbers: 52.25Fi, 52.35Ra, 52.65Tt

A striking phenomenon found in magnetic confinement fusion experiments is intrinsic or spontaneous rotation, namely, toroidal plasmas can self-organize and develop rotation without an external torque [1, 2], which plays a critical role in determining overall plasma rotation. In future large size burning plasmas such as ITER, intrinsic rotation may dominate because the use of neutral beams which, in present toroidal devices, offer a major momentum source for driving toroidal rotation while heating plasma, becomes extremely challenging. Therefore, understanding this complex, mostly non-diffusive transport phenomenon of intrinsic rotation is a key to predicting plasma flow in ITER. An optimized plasma flow is believed to play a critical role both in controlling macroscopic plasma stability, and in reducing energy loss due to plasma microturbulence.

Recently, extensive and intensive experimental studies have been carried out on this topic. The parametric dependence of the intrinsic rotation has been statistically characterized using a broad range of experimental data bases obtained in multiple machines. Specifically, the increment of central intrinsic rotation is shown to increase with the increment of plasma stored energy and to scale with the inverse of the plasma current [3] (the so called Rice scaling). Similar empirical scaling is also observed in other devices including JT-60U [4] and LHD [5], where the intrinsic rotation velocity is shown to increase with the ion pressure gradient in core plasmas with an internal transport barrier. There is no doubt that these results are important for making a qualitative projection of plasma rotation in ITER. A more fundamental, critical issue is to understand the underlying physical origins of the experimental empirical scalings. In this letter, global gyrokinetic simulations are used to address this issue.

Systematic global gyrokinetic simulations using experimentally relevant parameters have revealed an important nonlinear flow generation process due to the residual stress (a non-diffusive component of the momentum flux which is different from a pinch) produced by electrostatic turbulence of ion temperature gradient modes (ITG) and trapped electron modes (TEM) [6, 7]. Both fluctuation intensity and intensity gradient were identified to drive residual stress via wave-particle resonant interaction [8] in the presence of broken symmetry in the parallel wavenumber spectrum. Concerning the origin of the symmetry breaking, which is a critical ingredient for parallel (and toroidal) flow generation by turbulence, turbulence self-generated low frequency zonal flow shear has been identified to be a key, general mechanism in various turbulence regimes.

The turbulence driven residual stress, acting as an intrinsic torque, is shown to spin up toroidal rotation effectively. In our previous study, ITG turbulence driven intrinsic torque was shown to increase close to linearly with ion pressure gradient [7], in qualitative agreement with empirical trends obtained in various ion transport dominated experiments [3–5]. For certain plasma parameters, collisionless TEM (CTEM) turbulence can be a major source to drive multiple-channel transport, including toroidal momentum transport. However, the momentum transport and flow generation phenomena have not been well explored experimentally in the electron transport dominated regimes. Quantifying the characteristic dependence of turbulence generated toroidal flow in the electron turbulence regimes is particularly important for ITER experiments in which the electron channel is expected to dominate plasma transport.

First, we explore the relationship between the turbu-

lent residual-stress-induced intrinsic torque and the electron profile gradients in the CTEM-dominant regime. Our global turbulence simulations are carried out using the Gyrokinetic Tokamak Simulation (GTS) code [9]. Specifically, for CTEM simulations, ion dynamics is governed by the nonlinear gyrokinetic equation and electrons are treated as fully drift kinetic [7, 9]. The plasma momentum is mostly carried by ions because of large i-e mass ratio, but is substantially affected by electron dynamics via the quasineutrality condition. For this parametric scan study, radial profiles of electron density, temperature, and pressure gradient used in the simulations are specified according to the expression: $R_0/L_{n_e,T_e,p_e} = -\kappa \exp(-[(\rho-\rho_c)/0.28]^6)$, along with a fixed density/temperature/pressure at the center $\rho_c = 0.5$. This gives a fairly uniform CTEM drive in a region centered at ρ_c, and near zero gradient elsewhere. Absorbing boundary conditions are used by applying a damping effect in very narrow boundary layers at $\rho > 0.8$ and $\rho < 0.2$, which work to remove fluctuations coming from the unstable core region that touch the boundaries. The simulation scan is performed by varying the κ value. For all these simulations, plasmas are initially rotation-free and momentum-source-free, which allows us to concentrate on the residual stress and associated intrinsic torque. Note that the turbulence equipartition (TEP) momentum pinch [10], which should exist for CTEM turbulence with finite rotation velocity, is not examined in this letter since it does not contribute to the net flow generation due to the intrinsic torque. An equilibrium $\mathbf{E}\times\mathbf{B}$ shear that has been known to induce $k_\parallel$ symmetry breaking [11, 12] is also included via the radial force balance relation, which, however, is seen to be a minor player compared to CTEM self-generated zonal flows. The numerical MHD equilibrium used in this study corresponds to a real DIII-D discharge. All simulations in this paper use 100 particle/cell·species.

Instead of calculating the local torque $\nabla\cdot\mathbf{\Gamma}_\phi^{\rm RS}$ associated with residual stress $\Gamma_\phi^{\rm RS}$, we examine the rate of total toroidal momentum generation, dP_ϕ/dt. The quantity dP_ϕ/dt is a measure of the volume-integrated torque (or spatially averaged torque density) driven by turbulence, which has better correspondence to the intrinsic torque inferred from experiments or measured central intrinsic rotation. The simulation results for intrinsic torque density as calculated from dP_ϕ/dt, versus the electron pressure gradient ∇p_e, are summarized in Fig. 1, in which three curves correspond to three different cases of free energy for driving CTEM. The dominant free energy sources are ∇n (black), ∇T_e (green) and a combination of both (red), respectively. For all three cases, the intrinsic torque associated with nonlinearly generated residual stress is found to increase close to linearly with the electron pressure gradient. In other words, a larger central intrinsic rotation is expected to be produced in a plasma with a higher electron pressure gradient. The dominant underlying physics governing this scaling is rather straightforward, namely, both the turbulence intensity and the zonal flow shear, which are two key ingredients for driving residual stress, increase with the CTEM drive R_0/L_{p_e}. Moreover, the observation of the black curve being above the green and red curves indicates that the free energy in the density gradient is more efficient than that in the temperature gradient in driving intrinsic rotation via CTEM turbulence. One robust feature of CTEM driven intrinsic rotation is also highly remarkable, namely, the intrinsic rotation is generated mostly in the co-current direction, which is consistent with the trend of experimental observations in H-mode plasmas [3]. These results predicted from the gyrokinetic simulations suggest a strong connection between intrinsic rotation and electron parameters, which may have important implications, particularly for ITER experiments. It will be highly interesting to test this prediction in electron transport dominated experiments, such as NSTX. In comparison, the typical intrinsic torque density inferred from DIII-D experiments is on the order of unity ($\mathrm{Nm/m^3}$) [14].

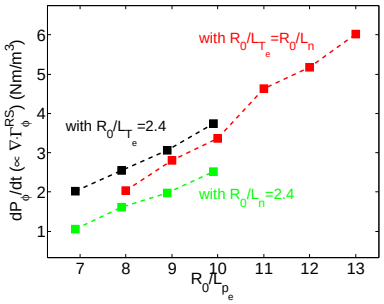

FIG. 1: CTEM-driven intrinsic torque density (spatially averaged) versus electron pressure gradient R_0/L_{p_e}.

Now we turn to exploring the dependence of turbulence driven residual stress and intrinsic rotation on the plasma current I_p. Again, this simulation study is carried out for CTEM turbulence. The primary purpose is to attempt to shed light on the physics origin of the current scaling which was obtained in multiple devices [3]. For this simulation study we adopt a similar methodology to that used in experiments for various investigations of current scans. A set of simulation experiments is carried out by holding the vacuum (external) magnetic field and plasma pressure profile fixed, while varying the plasma current. Specifically, this is accomplished by generating a series of shaped, numerical equilibria with $I_p = 0.75$, 1.0, 1.5 and 2.0 MA, using an MHD code.

The plasma gradients used for this study are: $R_0/L_{T_e} = R_0/L_n = 6$ and $R_0/L_{T_i} = 2.4$ with $T_e/T_i = 1.2$. Simulation results presented in the top-left panel of Fig. 2 show that the rate of toroidal momentum generation by CTEM turbulence increases close to linearly with the inverse of the plasma current. This result indeed re-

produces the same trend as that of the Rice scaling. It is highly interesting to compare this result for toroidal momentum transport with those for CTEM-driven heat and particle transport. Simulation results (not displayed in this letter) show that CTEM driven heat/particle fluxes are nearly at the same levels for the four cases. In other words, turbulent particle and electron heat transport are roughly independent of the plasma current in this scan, in contrast to the intrinsic torque. Apparently, our work presented here does not address the well-known, long standing mystery regarding the I_p-dependence of global energy confinement time typically observed in ion thermal transport dominated plasmas, for which the underlying origin might have to do with edge dynamics.

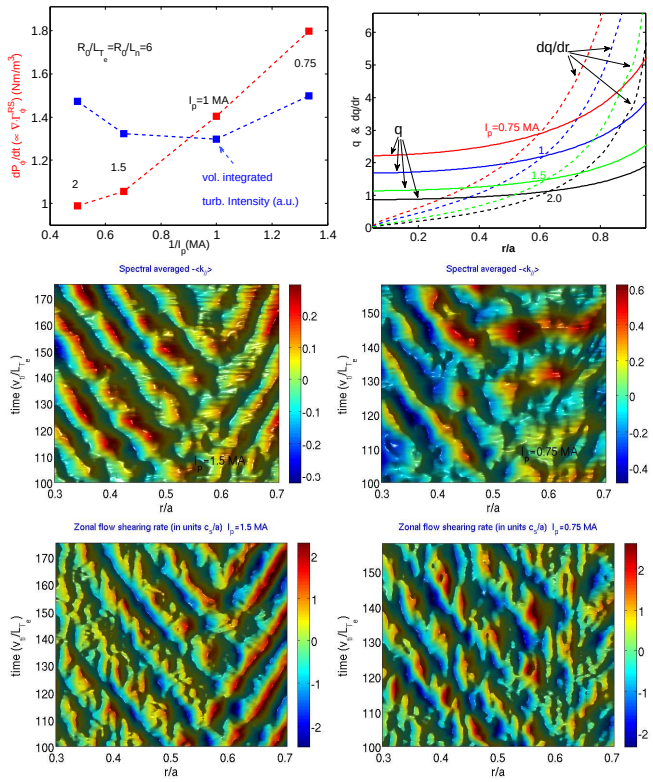

FIG. 2: CTEM-driven total intrinsic torque and volume-integrated turbulence intensity at steady state versus plasma current I_p (top-left) and radial profiles of q and dq/dr of the four equilibria used in this scan (top-right); spatio-temporal evolution of spectrum-averaged $\langle k_\| \rangle$ for two cases with I_p = 1.5 MA (middle-left) and I_p = 0.75 MA (middle-right); and spatio-temporal evolution of zonal flow shearing rate for $I_p = 1.5$ MA (bottom-left) and $I_p = 0.75$ MA (bottom-right).

With respect to the torque versus ∇T, ∇n and ∇p scaling in ITG and CTEM turbulence, the underlying physics governing the current scaling is less transparent. First, we examine the turbulence intensity levels of four cases. As is also shown in the top-left panel of Fig. 2, the volume-integrated turbulence intensities in the steady state are actually at the same level for the four cases, roughly independent of the current. This is consistent with the results of the simulated heat and particle fluxes whose magnitudes, in general, are believed to be more primarily coupled with the fluctuation intensity than other turbulence related quantities, and thus are insensitive to variation in the plasma current also. At the same time, the turbulence intensity gradient, which can also contribute to driving residual stress with an asymmetric fluctuation spectrum in parallel wavenumber $k_\|$ due to turbulence wave radiation induced wave momentum diffusion [13], does not show significant current dependence that can account for the torque vs I_p scaling observed in our simulations either. Hence, these results imply that the underlying physics for the current scaling has to do with the symmetry breaking dynamics and the associated mechanisms. This critical point is further directly elucidated by examining the amplitude of spectrum-averaged $\langle k_\| \rangle$, which serves as a quantitative measurement for how strongly the $k_\|$ symmetry is broken [6]. The results for two cases with I_p = 1.5 MA and I_p = 0.75 MA are presented in the middle panels of Fig. 2, which, as clearly indicated by the color bars, show that the overall amplitude of $\langle k_\| \rangle$ in the primary region of CTEM fluctuations is significantly increased (by a factor of $\gtrsim 2$) as the plasma current is halved. Consistent with the enhanced $k_\|$ symmetry breaking, the CTEM generated intrinsic torque is roughly doubled from the I_p = 1.5 MA case to the 0.75 MA case.

Now, the key issue is what makes the difference in the symmetry breaking when varying the plasma current. As we found previously, the turbulence self-generated zonal flow shear provides a general mechanism for the symmetry breaking. The $\mathbf{E} \times \mathbf{B}$ shearing rates of zonal flows corresponding to the above two cases with different I_p values, however, are very comparable, as illustrated in the bottom panels of Fig. 2. The color bars clearly show that the zonal flow shearing rates are on the same level. This indicates that the difference generated in the symmetry breaking level is not associated with the change in zonal flow shear. While zonal flow shear is a common element providing symmetry breaking in $k_\|$, our previous simulations also indicate the existence of other mechanisms beyond $\mathbf{E} \times \mathbf{B}$ shear for symmetry breaking. These include the radial variation of the safety factor, to be discussed below.

Note that, on the other hand, the corresponding q profile is remarkably boosted in the four equilibria as the plasma current is decreased from 2MA to 0.75MA; so is its radial variation, dq/dr (the top-right panel of Fig. 2). Also note that the parameter $\rho_*(\equiv \rho_i/a)$ for the four cases is roughly the same, i.e., $a/\rho_i \sim 170$, which is in the DIII-D range. This observation is highly suggestive that the current scaling of intrinsic torque and rotation may have connections with the change in the value of q and/or its radial variation.

To isolate the effect of safety factor from that due to

the radial variation of q, further computational experiments are performed. First, we examine the effect of the q value. To this end, three MHD equilibria are created, which hold the profile of dq/dr (and plasma pressure) fixed while boosting the q profile. For this scan, the CTEM driven intrinsic torque is found to decrease with the increase in the q value; so does the volume-integrated turbulence intensity, which appears to be a major cause for the observed intrinsic torque vs q dependence. The key point of this interesting result, however, is that the dependence of the torque on the q value shows the opposite trend to the current scaling obtained in Fig. 2.

Now we turn to exploring the effects of the radial variation of q on the intrinsic torque. To this end, three MHD equilibria are created, which hold the radially averaged q value nearly fixed in the central core region where CTEM turbulence is generated, but allow minor variation in the q profile in order to create significant variation in dq/dr, as illustrated in the upper-right panels of Fig. 3. At the same time, the plasma pressure is held fixed. Note that a normal (positive) magnetic shear is present in all equilibria used in this paper. The result of this simulation scan is presented in the upper-left panel of Fig. 3, which shows that the spatially averaged intrinsic torque density increases nearly linearly with dq/dr. On the other hand, the volume-integrated fluctuation intensity exhibits a much weaker dependence on dq/dr, which indicates that the observed intrinsic torque vs dq/dr scaling mostly results from the effect of the $k_\parallel$ symmetry breaking physics. Indeed, this is directly clarified by the results for the spectrum-averaged $k_\parallel$ presented in the lower panels of Fig. 3, which show that the amplitude of $\langle k_\parallel \rangle$ for $dq/dr(\text{central} - \text{averaged}) = 2.2$ is significantly higher than for $dq/dr = 0.9$, indicating enhanced $k_\parallel$ symmetry breaking with increased radial variation of q. Note the simple relation $k_\parallel = (nq - m)/qR \simeq (n/qR)(dq/dr)(r - r_0)$, near a rational surface at r_0. If we assume that the turbulence intensity is a good measure of average $\langle (r - r_0) \rangle$, the radial correlation length, $\langle k_\parallel \rangle \propto dq/dr$ is readily expected from this simple relation. Therefore, the observed enhancement of CTEM driven intrinsic torque is caused by the enhancement of $k_\parallel$ symmetry breaking with increased dq/dr.

The key point of this result is that the dependence of the intrinsic torque on dq/dr indeed produces the right trend which is consistent with the current scaling obtained in Fig. 2. Therefore, given the distinct effects of varying the q value and dq/dr on intrinsic torque generation, it is concluded that the current scaling results from the effect of the nonuniform q profile on the turbulence spectrum, namely, the magnetic shear induced $k_\parallel$ symmetry breaking, which is enhanced with increased dq/dr. We should point out that the effect of the radial variation of q on the nonlinear residual generation and the associated key role of it behind the current scaling revealed by these gyrokinetic simulations should be tested/validated by experiments. To a certain extent, this can be done by revisiting the experimental data base from which the current scaling was abstracted.

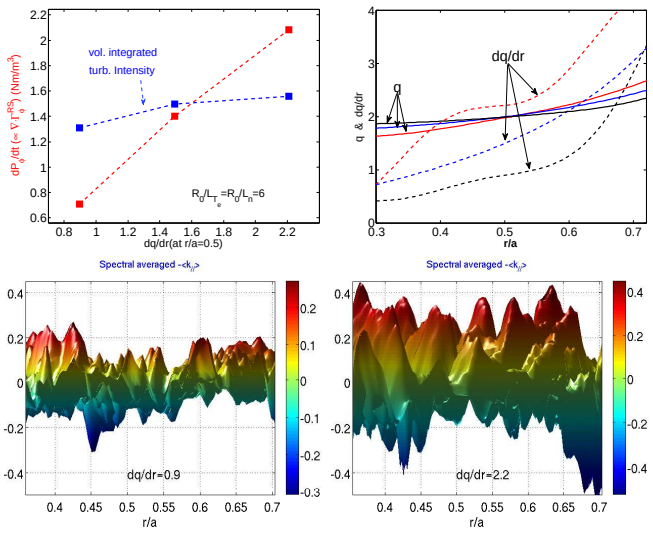

FIG. 3: CTEM-driven total intrinsic torque versus the radial variation of q averaged over the central core region (upper-left), corresponding radial profiles of q and dq/dr of the three equilibria used for these simulations (upper-right), and spatio-temporal images of spectrum-averaged $\langle k_\parallel \rangle$ for two cases with averaged $dq/dr = 0.9$ (lower-left) and $dq/dr = 2.2$ (lower-right) – these are 2D views in the $\langle k_\parallel \rangle$-$r$ domain.

Discussion with Dr. S. Kaye on experimental current scan studies is acknowledged. This work was supported by U.S. DOE Contract No. DE-AC02-09CH11466 and the SciDAC project for Gyrokinetic Particle Simulation of Turbulent Transport in Burning Plasmas.

* wwang@pppl.gov

[1] J. E. Rice *et al.*, Nucl. Fusion **44**, 379 (2004).
[2] J. S. deGrassie *et al.*, Phys. Plasmas **14** 056115 (2007).
[3] J. E. Rice *et al.*, Nucl. Fusion **47**, 1618 (2007).
[4] M. Yoshida *et al.*, Phys. Rev. Lett. **100**, 105002 (2008).
[5] K. Ida *et al.*, Nucl. Fusion **50**, 064007 (2010).
[6] W. X. Wang *et al.*, Phys. Rev. Lett. **102**, 035005 (2009).
[7] W. X. Wang *et al.*, Phys. Plasmas **17**, 072511 (2010).
[8] P. H. Diamond *et al.*, Phys. Plasmas **15**, 012303 (2008).
[9] W. X. Wang *et al.*, Phys. Plasmas **13**, 092505 (2006).
[10] T. S. Hahm *et al.*, Phys. Plasmas **14**, 072302 (2007).
[11] R. Dominguez and G. M. Staebler, Phys. Fluids, B **5**, 3876 (1993).
[12] O. D. Gurcan *et al.*, Phys. Plasmas **14**, 042306 (2007).
[13] P. H. Diamond *et al.*, Nucl. Fusion **49**, 045002 (2009).
[14] W. Solomon et al., Proc. of the 23nd IAEA Fusion Energy Conference, Daejon, Korea (IAEA, Vienna, 2010) (IAEA Report No. IAEA-CN-165/EX/3-5, 2010).